⌘ *Author's Choice*

THE JOURNAL OF BIOLOGICAL CHEMISTRY VOL. 286, NO. 14, pp. 12389–12396, April 8, 2011

Monitoring Surface Chemical Changes in the Bacterial Cell Wall

MULTIVARIATE ANALYSIS OF CRYO-X-RAY PHOTOELECTRON SPECTROSCOPY DATA[S]

Received for publication, December 6, 2010, and in revised form, February 16, 2011 Published, JBC Papers in Press, February 17, 2011, DOI 10.1074/jbc.M110.209536

Madeleine Ramstedt[‡1], **Ryoma Nakao**[§¶2], **Sun Nyunt Wai**[§2], **Bernt Eric Uhlin**[§2], **and Jean-François Boily**[‡3]

From the [‡]*Department of Chemistry and the* [§]*Department of Molecular Biology and The Laboratory for Molecular Infection Medicine (MIMS) Sweden, Umeå Centre for Microbial Research (UCMR), Umeå University, SE-90187 Umeå, Sweden and the* [¶]*Department of Bacteriology, National Institute of Infectious Diseases, 162-8640 Tokyo, Japan*

Gram-negative bacteria can alter the composition of the lipopolysaccharide (LPS) layer of the outer membrane as a response to different growth conditions and external stimuli. These alterations can, for example, promote attachment to surfaces and biofilm formation. The changes occur in the outermost layer of the cell and may consequently influence interactions between bacterial cells and surrounding host tissue, as well as other surfaces. Microscopic analyses, fractionation of bacterial cells, or other traditional microbiological assays have previously been used to study these alterations. These methods can, however, be time consuming and do not always give detailed chemical information about the bacterial cell surface. We here present an analytical method that provides chemical information on the outermost portion of bacterial cells with respect to protein, peptidoglycan, lipid, and polysaccharide content. The method involves cryo-x-ray photoelectron spectroscopy analyses of the outermost portion (within ~10 nm of the surface) of intact bacterial cells followed by a multivariate curve resolution analysis of carbon spectra. It can be used as a tool for characterizing and monitoring variations in the chemical composition of bacterial cell walls or of isolated outer membrane vesicles, variations that result from *e.g.* mutations or external stimuli. The method enabled us to predict accurately the alterations in polysaccharide content and surface chemistries of a set of well characterized *Escherichia coli* LPS mutants. The described approach may moreover be applied to monitor surface chemical composition of other biological samples.

Bacterial interactions with their surrounding environment are largely controlled by interactions between the cell wall and other surfaces. Thus, chemical composition and structure of the cell wall are of particular importance and may determine the nature of different interactions with surfaces such as host cells membranes or to abiotic surfaces. Gram-negative bacteria have cell walls containing a periplasm and an outer membrane. The periplasm includes a peptidoglycan layer as well as periplasmic proteins. The outer membrane phospholipid bilayer has lipopolysaccharides (LPS) exposed from its outer layer, and it contains miscellaneous outer membrane proteins (1). Some bacterial species have capsular polysaccharides outside the outer membrane, which is regarded as one of virulence factors. However, the commonly used laboratory strains of *Escherichia coli* (*e.g. E. coli K-12* derivatives) do not produce capsular polysaccharides. The LPS exhibits considerable variations between bacterial species and represents a highly dynamic part of the bacteria. Bacterial pathogens have common response mechanisms enabling them to modify protein and LPS components of the outer membrane in response to stressful environments (for example in a phagosome) (2). Recent studies have also shown that alterations in the LPS structure may distinctly influence cell surface hydrophobicity, biofilm formation, as well as interactions with antibacterial substances such as tobramycin, streptomycin, amikacin, and gentamicin[4] (4–7). Monitoring such changes in cell wall compositions, however, involves elaborate and time-consuming procedures.

In this article we describe an efficient approach for characterizing and monitoring chemical alterations of bacterial cell walls using cryo-x-ray photoelectron spectroscopy (cryo-XPS)[5] and multivariate curve resolution analysis. XPS is a surface-sensitive analysis technique that is widely used to determine the chemical composition of the surface layer, including those of biological materials. Because the technique is surface-sensitive, it monitors only the bacterial cell wall and consequently offers a unique advantage over many other techniques. Furthermore, it can be performed on intact bacterial cells, thereby reducing lengthy extraction procedures and the risk of introducing some bias or sample treatment artifacts into the dataset.

XPS has also been used earlier for bacterial cell wall studies (8, 9, 11, 13) and indicated organic compositions on the basis of ratios between different group functionalities. This work has however mostly required the use of freeze-dried or desiccated bacterial samples and of standard samples, as the technique involves analyses under high vacuum. For example, Rouxhet *et al.* constructed a system of equations to estimate the content of peptide, polysaccharides, and hydrocarbons in cell walls of freeze-dried Gram-positive bacteria (and in food products) (8–10). Although this approach does provide reasonable

[S] The on-line version of this article (available at http://www.jbc.org) contains supplemental Figs. S1 and S2, Tables S1 and S2, a section on FTIR analyses, additional references, and a Matlab file.

⌘ *Author's Choice*—Final version full access.

[1] Supported by the Curth Nilsson Foundation for Scientific Research. To whom correspondence should be addressed: Dept. of Chemistry, Umeå University, SE-90187 Umeå, Sweden. Tel.: 46-90-786-6328; Fax: 46-90-786-7655; E-mail: madeleine.ramstedt@chem.umu.se.

[2] Supported by grants from the Swedish Research Council.

[3] Supported by the Swedish Research Council as well as the Wallenberg and Kempe foundations.

[4] R. Nakao, M. Ramstedt, S. N. Wai, and B. E. Uhlin, unpublished data.

[5] The abbreviations used are: cryo-XPS, cryo-x-ray photoelectron spectroscopy; OMV, outer membrane vesicle.

results, it can be highly sensitive to peak-fitting procedures. Another point of concern for such XPS studies is the possibility of sample alterations due to drying (11). However, more recent generations of currently available spectrometers provide possibilities of analyzing samples at liquid nitrogen temperatures. If samples are quickly frozen before exposure to vacuum and then kept frozen throughout the measurement period, the analysis will consequently take place with the water still present in the sample structure (12,13). This approach minimizes structural changes in the samples and consequently provides a means of analyzing bacterial surfaces under a more physiologically relevant form, albeit frozen (13). Low temperatures also minimize sample degradation by the x-ray beam. Furthermore, because the analysis only requires that the sample be rinsed (to remove soluble media components) and centrifuged, it circumvents time-consuming drying procedures which can lead to additional alterations and contaminations (11). However, because the presence of water in the frozen samples impedes previous quantification using element ratio methods, an alternative approach was needed to easily extract sugar, protein, peptidoglycan and lipid contents.

This paper presents a method for quantifying the composition of the bacterial cell walls using multivariate spectral analysis of cryo-XPS spectra as applied to a set of well characterized laboratory strains of *E. coli* representing LPS mutants with a range of surface compositions. We show how XPS can be used to extract cell wall composition and discuss the general applicability of this method for monitoring chemical changes in surfaces of bacteria and outer membrane vesicles (OMVs). The model parameters and Matlab code are supplied in the supplemental material. The method relies on access to XPS instrumentation which is commonly available in surface analysis laboratories. This instrumentation has not previously been used extensively for biological samples. However, with the development of new methodologies (like the one described in this article) we expect that the use of this technique for studies of biological specimens will increase.

EXPERIMENTAL PROCEDURES

Short Overview of XPS Multivariate Curve Resolution—XPS measures the kinetic energy of electrons emitted from surfaces under x-ray radiation. By knowing the energy of the incoming x-ray beam and measuring the kinetic energy of electrons leaving the surface, binding energy is obtained by the spectrometer. Binding energy is specific to both elements and electronic orbitals from which electrons originate. It is also sensitive to the chemical environment of the atoms at the surface. The so-called C 1s spectrum of carbon, for example, may encompass binding energies specific to carbon in an aliphatic hydrocarbon chain or in a carboxylate group. Functional groups present may consequently be identified using this approach. The analysis depth depends on the sample nature and is determined by the so-called escape depth of the electron, namely the distance an electron can travel through the sample without losing its specific kinetic energy. Generally, for biological samples this depth is about 10 nm. Moreover, as the escape depth decays exponentially from the surface and down into the sample, the majority

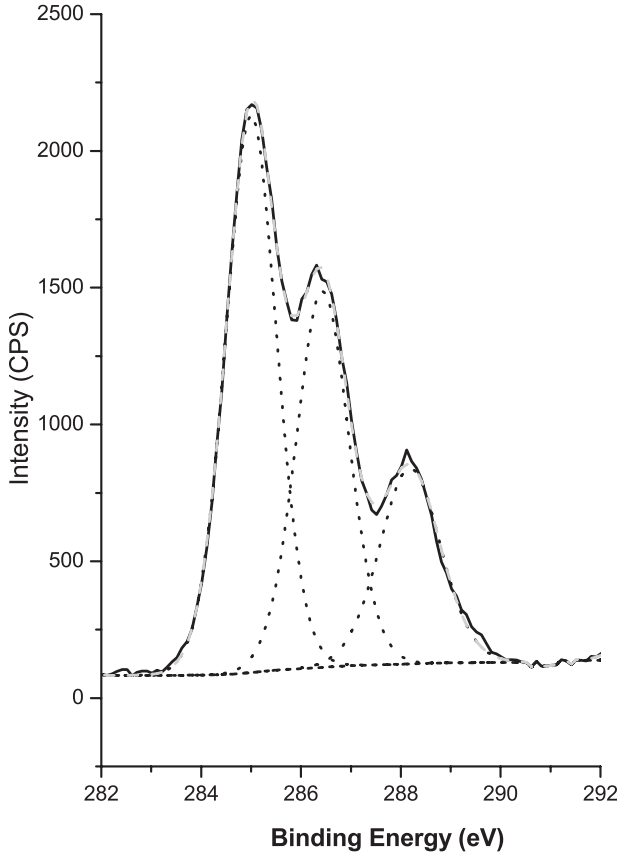

FIGURE 1. **Typical C 1s spectrum of Gram-negative cell wall (here the *E. coli* wild type, BW25113) showing traditional fitting using Gaussian-Laurentian peak shapes for aliphatic carbon (at 285.0 eV), carbon bound to one oxygen or nitrogen atom (at 286.6), and carbon bound to two oxygen or an oxygen and a nitrogen (at 288.3 eV).** The raw data are represented by a *solid black line*, the different components with *dotted lines*, and the fit of the model to the data is represented by the *gray broken line*.

(63%) of the signal will originate from about one-third of the analysis depth (14).

Because the cell wall of bacteria consists of polysaccharides, lipids, proteins, and peptidoglycan, we expect to see functional groups belonging to these substances in XPS spectra. From the fine structure of the carbon peak (Fig. 1), it is possible to extract information on the content of aliphatic carbon, carbon atoms bound to one oxygen or one nitrogen, and carbon atoms bound to more than one oxygen and/or nitrogen by using curve-fitting procedures. However, unique solutions are often achieved with difficulty in spectra consisting of highly overlapping peaks because they require simultaneous determinations of multiple sets of adjustable parameters (*e.g.* binding energy, peak half-width maximum, function shape, etc.). The multivariate curve resolution approach, used in this study, provides a more consistent and objective way to analyze these data. Simply stated, it reduces common features from XPS spectra of varied compositions into a small set of spectral components. These components can be used to reproduce the spectra accurately by multiplication with their respective relative concentrations, much like in the Beer-Lambert law used in spectrophotometry. In this study we produce three distinct components for peptides, lipids, and polysaccharide common to a wide range of bacterial cells. These components can be used to extract relative concen-

TABLE 1
Bacterial strains used in this study

Strain/plasmid	Relevant genotype or phenotypes or selective marker[a]	Source and/or reference
***E. coli* strains**		
BW25113	Wild type, K12 strain, *lacI*^{q} *rrnB*$_{T14}$ Δ*lacZ*$_{WJ16}$ *hsdR514* Δ*araBAD*$_{AH33}$ Δ*rhaBAD*$_{LD78}$	NIG collection (Japan) 28
RN101	Δ*waaC*, BW25113 derivative, heptose-less LPS. Km^{r} cassette was removed	Footnote 4
RN102	Δ*hldE*, BW25113 derivative, heptose-less LPS. Km^{r} cassette was removed	Footnote 4
RN103	Δ*waaF*, BW25113 derivative, inner-core mutant LPS contains 2 KDO and 1 heptose. Km^{r} cassette was removed	Footnote 4
RN104	Δ*waaG*, BW25113 derivative, core mutant LPS which lacks outer core. Km^{r} cassette was removed	Footnote 4
RN105	Δ*waaL*, BW25113 derivative, no O-antigen LPS. Km^{r} cassette was removed	Footnote 4
RN106	Δ*waaP*, BW25113 derivative, dephosphorylated LPS. Km^{r} cassette was removed	Footnote 4
RN107	Δ*galE*, BW25113 derivative, LPS lacking galactose. Km^{r} cassette was removed	Footnote 4
RN115	*flhD*::Tn*5*, *waaL* derivative, flagella mutant, Km^{r}	This study
***Vibrio cholerae* strains (for vesicle samples)**		
V5:/04	non-O1 non-O139 clinical isolate (2004)	Swedish Institute of Infectious Diseases
V5:/04 Δ*hapR*	Δ*hapR*, V5;/04 derivative	29
P27459	O1 Inaba, El Tor clinical isolate (1976, Bangladish)	30
Plasmids		
pNTR-S.D.	ColE1 derivative, 8.4 kb, Amp^{r}	National BioResource Project (National Institute of Genetics, Japan) (3)
pNT3(*hldE*)	pNTR-SD derivative containing *hldE* gene under *tac* promoter, utilized for complementation of *hldE* gene, Amp^{r}	National BioResource Project (National Institute of Genetics, Japan) (3)

[a] Amp^{r}, ampicillin resistance, Km^{r}, kanamycin resistance.

trations of these three substances in the samples considered in this study. They could also, potentially, be used to extract these concentrations in other chemically related samples.

XPS—We used a range of LPS mutants from *E. coli* strain BW25113 with differences in polysaccharide composition (Table 1) (4). The bacteria were collected from fresh colonies on plates grown at 37 °C for 17 h. The samples were then washed twice by PBS, centrifuged, and placed on a sample holder as wet pellets for XPS analysis. The volume of the pellet on the holder was 20 μl. The sample holder contains a metallic grid to ensure efficient freezing and attachment. The holder was directly placed on the precooled transfer rod (−170 °C) in the loading chamber of the spectrometer under an atmosphere of dry N_2(g) where the cells were frozen within 10–15 s. The chamber was thereafter evacuated to below a pressure of 10^{-6} torr, and the sample was transferred to the analysis chamber. XPS spectra were collected on cells kept at −155 °C (and pressure $<10^{8}$ torr) with a Kratos Axis Ultra DLD electron spectrometer using monochromated Al Kα source operated at 150 W. Analyzer pass energy of 160 eV was used for acquiring survey spectra and 20 eV for acquiring spectra of individual photoelectron lines. The analysis area was 0.3 × 0.7 mm. The spectrometer charge-neutralizing system was used to compensate for sample charging during the measurement, and the binding energy scale was referenced to the C 1s aliphatic carbon peak at 285.0 eV. Thus, although some initial curve fitting of the spectra was necessary to adjust the binding energy scale it is not explicitly used in the multivariate analyses. The total analysis time for each bacterial sample was ~2.5–3 h including time for freezing and for pressure changes between vacuum and normal atmosphere.

We analyzed a total of 41 samples: 7 standards, 5 bacterial vesicle samples, 2 outer membrane samples, 27 bacterial samples. The standard samples were peptidoglycan from *Staphylococcus aureus* (Sigma, 77140), transferrin protein (Sigma, T2036) lysozyme protein (Sigma, 62970), lipid A from *E. coli* (Sigma, L6638), LPS from *E. coli* (Sigma, L6893) D-glucose (DBH Chemicals), and starch (Merck), all analyzed without further purification.

Sample Purity—Because XPS analyses are surface-sensitive they are also sensitive to surface contamination from the air or from sample handling. Generally, all samples analyzed with XPS will display a hydrocarbon contamination at the surface which originates from very low levels of *e.g.* pump oil in the air around the XPS. The level of this contamination depends on exposure time and on the surface properties of the material analyzed, but it can be expected to be higher on hydrophobic surfaces than on hydrophilic surfaces. Previous analyses using the fast freezing technique have showed very low levels of surface contamination due to the quick sample loading procedure and the relatively high content of water at the surface of the sample (12), the latter reducing the driving force for spontaneous deposition of hydrocarbon contaminations. Despite this, the presence of contaminations cannot be completely ruled out and can lead to overestimations of the content of aliphatic carbon in XPS samples. In the multivariate fitting this surface contamination will to some extent be "automatically" included because the deposition of contamination onto the substances in the samples should be similar to the deposition onto their respective pure standards. Furthermore, if the samples are measured following the low temperature procedure described here, no freeze-drying step is required before analysis, thereby reducing pretreatment efforts and reducing surface contamination (11).

Numerical Analyses—The XPS spectral lines of the C 1s region were analyzed and manipulated by chemometric methods coded in the computational language of Matlab (The Mathworks, Inc.). All spectra sets were expressed in a matrix **A** with one set of *m* rows of binding energies pertaining to all *n* columns of measurements. Measurements collected at different ranges and/or intervals of binding energies were interpolated to one single set of values along *m* in the 281–291 eV range. All relative intensity values were offset to zero absorbance values at

291 eV and normalized for area by numerical integration. The number of chemically relevant vectors contributing to the variance of **A** was estimated by analysis of results of a singular value decomposition (15). The dominant three vectors reproduced 99.7% of the variance of the data and were used to produce matrix $\mathbf{A}_{net}$. This matrix was analyzed by multivariate curve resolution (MCR) analysis with the program MCR-ALS (16). The calculations produced pure spectral components ($\boldsymbol{\epsilon}$) common to each sample as well as concentration profiles (**C**) that were used to reproduce $\mathbf{A}_{net}$ such that $\mathbf{A}_{net} = \boldsymbol{\epsilon}\mathbf{C}+\mathbf{E}$, where **E** is the deviation of the model to the data. The resulting percentages obtained from the model correspond to percentage of the carbon peak, *i.e.* the model presents molar percentage of carbon atoms from each substance, of the total molar percentage of carbon at the surface. To relate to the molar percentage of substance at the surface, the elemental composition of each substance has to be known as well as the total atom percent of C. However, due to the complexity of biological samples the exact elemental composition is difficult to obtain. For a pure standard protein (BSA), pure lipid (cholesterol), and pure sugar (glucose) the atom percent C of the surface (obtained by XPS theoretically) would be 63.0 atom %, 96.6 atom %, and 50.0 atom %, respectively. Thus, in a mixture with 30 molar % of each substance, the content of lipid will appear higher than that of protein and sugar in XPS spectra. The method developed can be used on any type of sample but will assume that only mixtures of peptides, lipids, and polysaccharides, contribute to the C 1s region. If other compounds containing carbon exist at the surface of the sample, they will not be described, and their contribution will be interpreted as peptide, lipid, and/or polysaccharide.

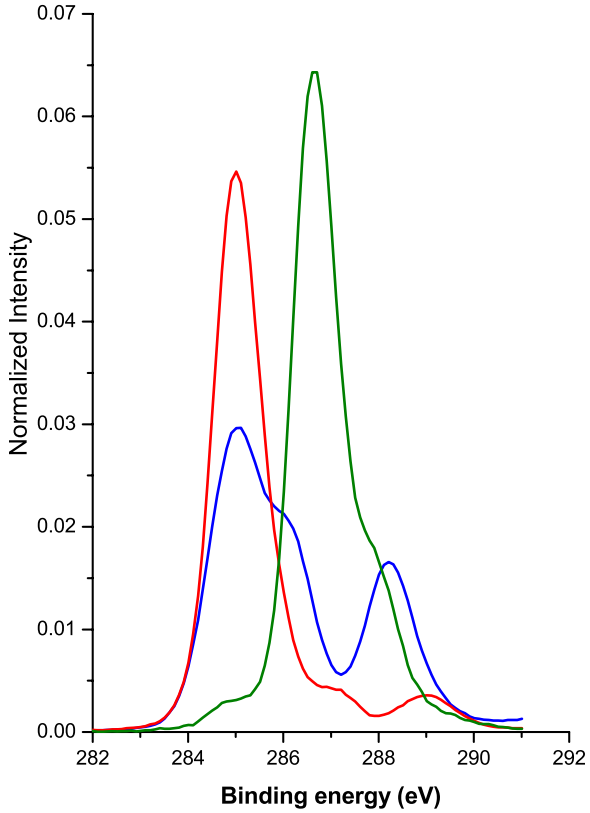

FIGURE 2. **Components obtained by the multivariate analysis.** A combination of these three components can explain the spectral variation of the complete dataset analyzed. The components are shown as component 1 (*blue*, peptide), component 2 (*red*, lipid), and component 3 (*green*, polysaccharide).

RESULTS

Spectral Components—An analysis of the dimensionality of the 41 spectra sets (supplemental Fig. S1 and supplemental Tables S1 and S2) confirmed that only three linearly independent components are required to account for 99.7% of the spectral variations. The three dominant singular value decomposition vectors were rotated to a real chemical space with MCR-ALS, yielding the three C 1s components of Fig. 2. Attempts at using fewer components did not satisfactorily reproduce the data whereas more components yielded chemically unrealistic components. Therefore, although we do recognize the complexity of the material under study, variations in the surface chemistry can be described in terms of three major components.

Investigation of these components showed that component 1 consisted of a peak at 285.0 eV, one shoulder at 286.1 eV and a well resolved peak at 288.1 eV. This component arises from an aliphatic carbon (*e.g.* -**C**H_2-CH_2-, generally at 285.0 eV) a carbon bound to one nitrogen (-**C**H_2-N<, generally at 286.11) and a carbon in a peptide bond (-N-**C** = O, generally at 288.1) (17). Component 1 consequently corresponds to protein and/or peptidoglycan. The second component consists of a large peak at 285.0 eV, a very small at 287.1 eV, and another small one at 289.1 eV and therefore arises from aliphatic carbon, a carbon single bonded to oxygen (286.4–287.0 eV) and a carbon in a carboxylic acid (289.3 eV) (17). This composition points to a lipid-like molecule with a carboxylic acid as one end group. The third component consists of a very small intensity at 285.0 eV, a large one at 286.7 eV, and a smaller shoulder at 288.0 eV. This corresponds well to a substance with low amounts of aliphatic carbon, larger amounts of carbon atoms bonded to one oxygen, as well as carbon atoms with ester or ether-type bonds (O-**C**-O, 287.9) (17). Thus the third component corresponds well to a polysaccharide.

Unfortunately, it was not possible to distinguish between the protein content and peptidoglycan content using this method because their spectra are too similar (Fig. 3). Instead, the first spectral component represents the content of both protein and (or) peptidoglycan in the samples analyzed, much like previous models (10), and this compound will subsequently be called the peptide component.

The experimental spectra of standard samples of proteins, sugars, and LPS were similar to the theoretical components obtained from our multivariate analysis. Some discrepancies were found and were thought to be due to the chemical complexity of the standard samples or impurities in the standards (Fig. 3) The purity of the standards was analyzed using infrared spectrometry. These analyses showed the presence of polysaccharide and amide bonds in the LPS and lipid A standards. They also indicated the presence of bonds in protein and peptidoglycan standards that could be interpreted as polysaccharide by the model. These results are presented and discussed further in the supplemental Fig. S2 and the supplemental FTIR analyses.

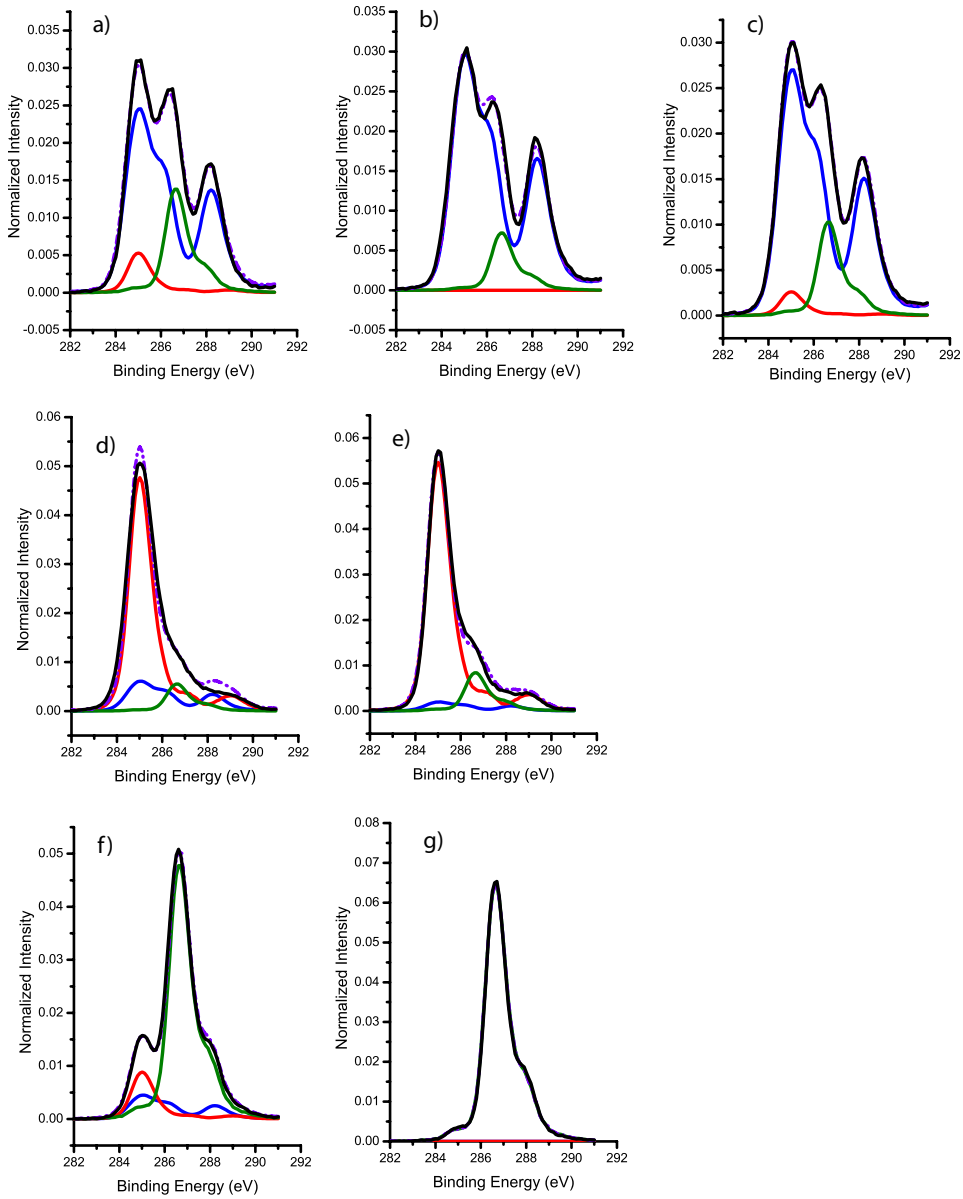

FIGURE 3. **Agreement among the multivariate components obtained from the spectral analysis (*purple broken line*) and experimental XPS spectra (*black line*) of standard samples of peptidoglycan (*a*), protein (*b* and *c*) in the form of lysozyme (*b*) and transferrin (*c*), LPS (*d*), lipid A (*e*), starch (*f*), and glucose (*g*).** The multivariate components are shown as lipid (*red*), peptide (*blue*), and polysaccharide (*green*).

Bacterial Samples—Our numerical analyses predict the spectra of all *E. coli* LPS mutant cell walls analyzed (Fig. 4*a*) on the basis of variations in the relative concentrations of our three components (Fig. 4*b*). Our estimated polysaccharide content corresponds well to expected values in the otherwise isogenic LPS mutants with different sugar content. Indeed, as the analysis depth is relatively constant, a thicker top polysaccharide layer could impede analysis of the deeper underlying lipid bilayer and result in an apparent lower content of lipid. Furthermore, previous studies have shown that mutants with decreased amounts of LPS have decreased protein content of the outer membrane but an increased amount of phospholipid (18, 19) which is reflected in Fig. 4*b*.

Our analyses were limited to the carbon spectra only to produce a simple and straightforward method. It is however evident that this method can be readily extended to any other spectral features and, for instance, may highlight correlations between peptide content and nitrogen at the surface. This can also be done by simply using the nitrogen content from the N 1s spectrum as a separate validation to our multivariate curve resolution analysis. Fig. 4*b* shows a good agreement between our spectral component of peptide and independently determined nitrogen content. A correlation between the nitrogen content and our modeled peptide content was also established for all 41 samples used for this study (Fig. 5). We chose not to include the nitrogen peak directly into our multivariate analysis because the nitrogen spectra did not, apart from the relative content, vary significantly between the different samples.

Finally, flagella-free *waaL* mutant and OMVs purified from this nonflagellated mutant were also analyzed to evaluate the validity of our spectral interpretations (Fig. 4*b*). These samples were chosen to see whether removal of flagella, a bulky protein-

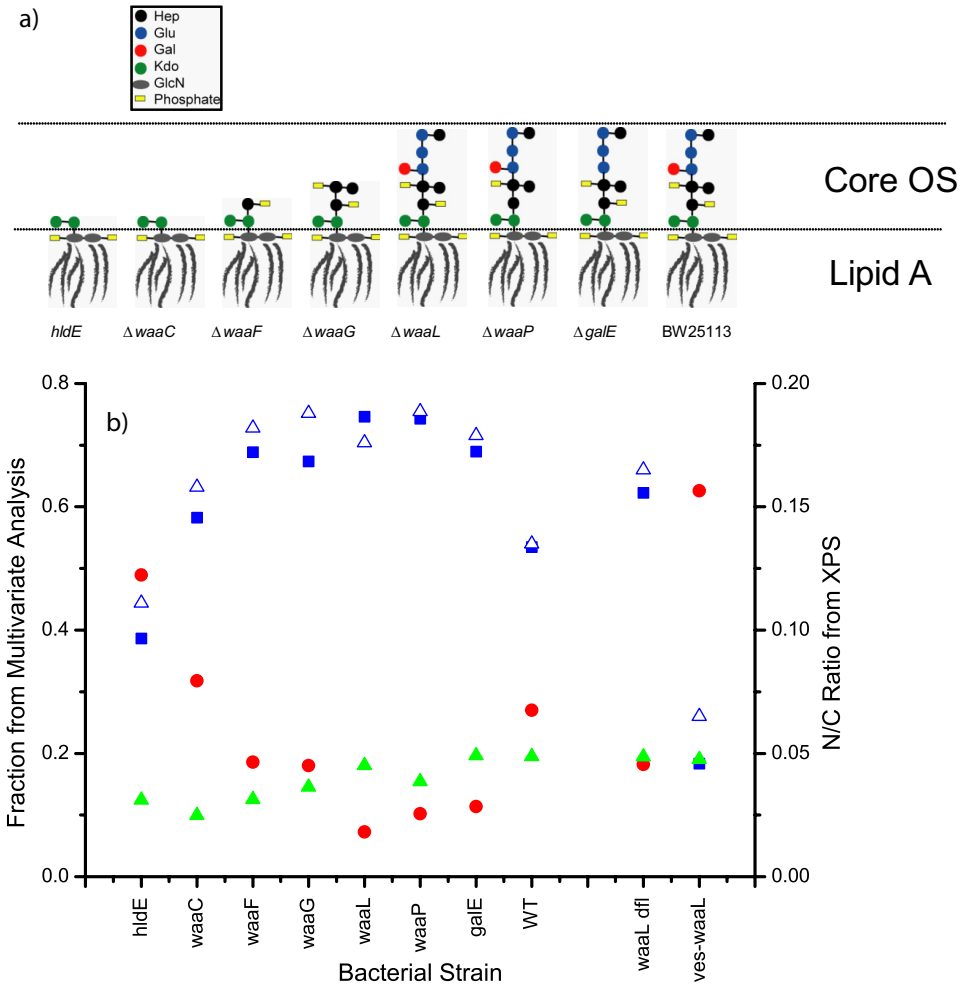

FIGURE 4. *a*, composition of cell wall for the LPS mutants. *b*, output from multivariate spectral analysis. *ves-waaL*, vesicle sample from *waaL* without flagella; *waaL dfl*, *waaL* without flagella. *Green triangles*, content of polysaccharide; *red circles*, content of lipids; *blue squares*, content of peptide, all from the multivariate spectral analysis. *Empty blue triangles* represent the amount of nitrogen relative to total carbon at the surface from XPS analysis.

aceous surface component, would enable a greater analysis depth into the lipid bilayer. Consistent with this hypothesis, the peptide content of the spectra decreased while the lipid increased in the mutant without flagella (Fig. 4*b*). In the OMV sample, the lipid content was higher than in the bacterial cell, and the protein/peptidoglycan content decreased down to the same level as the polysaccharide content. OMVs are formed from the outer membrane of bacterial cells and in general contain mainly LPS, phospholipids, membrane proteins, and some periplasmic components (20). Thus, a decreased amount of peptidoglycan (and perhaps also decreased amount of membrane proteins) in these vesicles could account for the large change in the peptide component compared with the bacterial cell surface. Such a decrease would result in a higher relative amount of lipid in the OMV than in the bacterial cell wall.

DISCUSSION

The analysis of standards and bacterial samples indicates that the model is capable of predicting the composition with respect to our three components. The agreement between the peptide component and the amount of nitrogen at the surface further indicates that the amount of peptide is well predicted. FTIR analyses of standard samples showed that the model may possibly overestimate polysaccharide content in, for example, glycol proteins or proteins that contain a large amount of for side groups containing C-O bonds. Our method nonetheless presents an advance in the chemical characterization of bacterial cell surfaces. Using the multivariate curve resolution analysis coupled with cryo-XPS analysis, we could readily monitor alterations that occur in the bacterial cell wall and understand how these changed the physical chemistry of the surface.

Previous research has shown that a decreased amount of polysaccharide and protein/peptidoglycan at the surface of the samples changed surface hydrophobicity and biofilm formation.[4] Using our new method, we can show how polysaccharide content changes between different mutants (Fig. 4*b*) and explain changes in surface hydrophobicity as an effect of variations in the content of hydrophobic lipids near the surface.[4] We can consequently confirm that XPS probes a part of the bacterial surface of outermost importance to the physical and chemical properties as indicated from measurements with other analysis techniques and assays. Component concentrations obtained in our approach consequently should improve our ability in understanding surface properties and in predicting bacterial interactions in a wide range of environments.

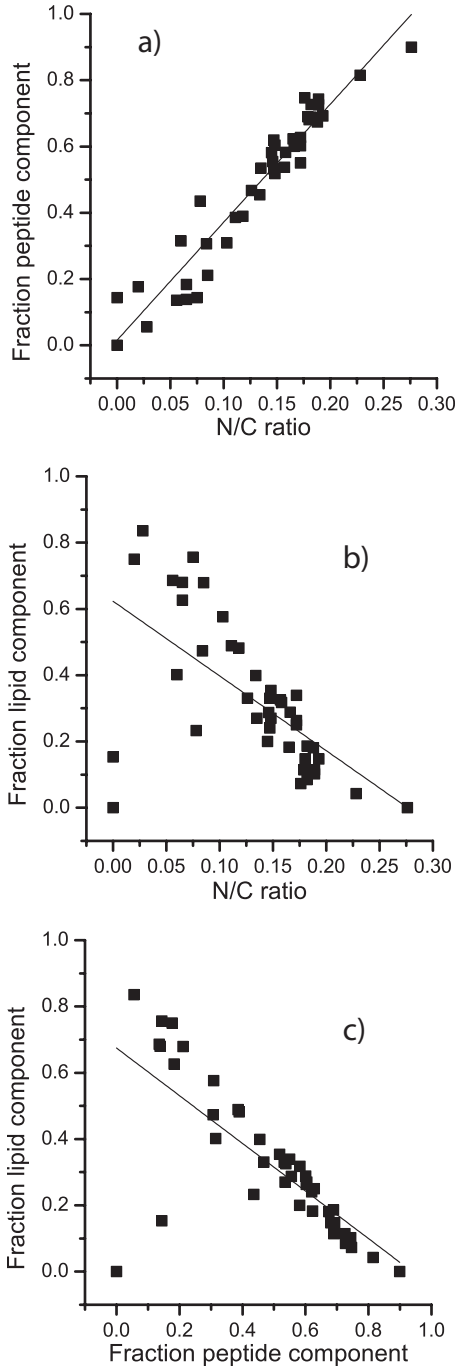

FIGURE 5. **Plots showing the correlation between the lipid and peptide components and the content of nitrogen at the surface.** *a*, clear correlation ($R^2 = 0.92$) between the content of nitrogen at the surface and peptide component. *b*, slight negative correlation between content of nitrogen and the lipid component ($R^2 = 0.38$). *c*, slight correlation between the lipid content and the peptide content ($R^2 = 0.54$). If the glucose and starch standards were removed the correlation in *b* and *c* R^2 became 0.80 and 0.95, respectively, but the correlation in *a* was not affected. The correlation in *b* is due to the negative correlation between the lipid content and the peptide content seen in *c*. No correlation existed between nitrogen and the sugar component ($R^2 = 0.024$, data not shown).

The analysis depth of the XPS analysis is less than 10 nm while the thickness of the Gram-negative cell wall has been described to be between 10 and 40 nm (21–23). Consequently, the analysis will not reach past the cell envelope and into the interior of the cell. For bacterial samples, the probing depth will be highly influenced by the presence and size of surface appendages, capsular polysaccharides, and the outer membrane composition. Especially the length of the variable structure of LPS influences the thickness of the cell walls. Atomic force microscopy has previously determined the LPS lengths of *E. coli* without O-antigen to be from 3 ± 2 to 5 ± 3 nm. The lengths of LPS in *E. coli* with O-antigen (three O157 and two O113 E strains) ranged from 17 ± 10 to 37 ± 9 nm (24). The BW25113 strain used in this study not only lacks the capsular polysaccharides but also the long O-antigen of LPS due to an IS*5* insertion in the *wbbL* gene involved in the O-antigen synthesis (25). The bilayer LPS-phospholipid structure of rough *Pseudomonas aeruginosa* (PAO1) has been modeled to be ~6–7 nm thick in total (26), and the thickness is likely to be similar in rough *E. coli*. Therefore, the described XPS analyses are considered to reach through the outer membrane into the periplasm with its peptidoglycan layer for the bacteria used in this study. In *E. coli* the peptidoglycan layer has been reported to be 6 nm in hydrated form (27), indicating that the inner cytoplasmic membrane most likely cannot be detected by the XPS. However, the drastic decrease in peptide composition between the bacterial and OMV samples from the *waaL* mutant indicate that the analysis depth does reach into the peptidoglycan layer for the bacteria analyzed here.

CONCLUSION

We have developed a method for obtaining the content of protein/peptidoglycan, lipid, and sugar in the surface layer of intact bacterial cells. This method enables efficient monitoring of variations in bacterial cell surface compositions in response to growth conditions and addition of antibiotics as well as other external stimuli.

The method can be used for chemical characterization and of bacterial samples without freeze-drying or damaging the cells with lengthy chemical analyses. The model was able to predict and compare the expected cell wall composition of a set of defined LPS mutants, and the peptide content showed good agreement with the experimental nitrogen content. This approach can consequently be readily used for extracting chemical composition of bacterial samples containing lipids, carbohydrates, and proteins/peptidoglycans, and it would also be easily applied to other complex biological samples. We hope that this method will become a useful tool for analyzing and comparing bacterial cell wall composition, *e.g.* in case of different bacterial mutants and OMVs.

Acknowledgments—We thank National BioResource Project (National Institute of Genetics, Japan) E. coli for providing plasmids and strains.

REFERENCES

1. Hancock, I. C. (1991) *Microbial Cell Surface Analysis* (Mozes, N., Handley, P. S., Busscher, H. J., and Rouxhet, P. G., eds) pp. 23–59, VCH Publishing, Inc., New York
2. Ohl, M. E., and Miller, S. I. (2001) *Annu. Rev. Med.* **52,** 259–274
3. Saka, K., Tadenuma, M., Nakade, S., Tanaka, N., Sugawara, H., Nishikawa, K., Ichiyoshi, N., Kitagawa, M., Mori, H., Ogasawara, N., and Nishimura, A. (2005) *DNA Res.* **12,** 63–68
4. Flemming, C. A., Palmer, R. J., Jr., Arrage, A. A., van der Mei, H. C., and

White, D. C. (1998) *Biofouling* **13,** 213–231
5. Sabra, W., Lûnsdorf, H., and Zeng, A. P. (2003) *Microbiology* **149,** 2789–2795
6. Kadurugamuwa, J. L., Lam, J. S., and Beveridge, T. J. (1993) *Antimicrob. Agents Chemother.* **37,** 715–721
7. Hoffman, L. R., D'Argenio, D. A., MacCoss, M. J., Zhang, Z., Jones, R. A., and Miller, S. I. (2005) *Nature* **436,** 1171–1175
8. Dufrêne, Y. F., van der Wal, A., Norde, W., and Rouxhet, P. G. (1997) *J. Bacteriol.* **179,** 1023–1028
9. Rouxhet, P. G., Misselyn-Bauduin, A. M., Ahimou, F., Genet, M. J., Adriaensen, Y., Desille, T., Bodson, P., and Deroanne, C. (2008) *Surface Interface Anal.* **40,** 718–724
10. Ahimou, F., Boonaert, C. J., Adriaensen, Y., Jacques, P., Thonart, P., Paquot, M., and Rouxhet, P. G. (2007) *J. Colloid Interface Sci.* **309,** 49–55
11. van der Mei, H. C., de Vries, J., and Busscher, H. J. (2000) *Surface Sci. Rep.* **39,** 1–24
12. Ramstedt, M., Shchukarev, A. V., and Sjöberg, S. (2002) *Surface Interface Anal.* **34,** 632–636
13. Leone, L., Loring, J., Sjöberg, S., Persson, P., and Shchukarev, A. (2006) *Surface Interface Anal.* **38,** 202–205
14. Hochella, M. (1988) in *Spectroscopic Methods in Mineralogy and Geology* (Hawthorne, F. C., ed) pp. 573–637, Mineralogical Society of America, Washington, D. C.
15. Golub, G. H., and Reinsch, C. (1970) *Numer. Math.* **14,** 403–420
16. Jaumot, J., Gargallo, R., de Juan, A., and Tauler, R. (2005) *Chemometr. Intell. Lab.* **76,** 101–110
17. Beamson, G., and Briggs, D. (1992) *High Resolution XPS of Organic Polymers: The Scienta ESCA300 Database*, Wiley, Chichester, UK
18. Smit, J., Kamio, Y., and Nikaido, H. (1975) *J. Bacteriol.* **124,** 942–958
19. Koplow, J., and Goldfine, H. (1974) *J. Bacteriol.* **117,** 527–543
20. Ellis, T. N., and Kuehn, M. J. (2010) *Microbiol. Mol. Biol. Rev.* **74,** 81–94
21. Metzler, D. E., and Metzler, C. M. (2001) *Biochemistry: The Chemical Reactions of Living Cells*, Vol. 2, Academic Press, San Diego, CA
22. Costerton, J. W., Ingram, J. M., and Cheng, K. J. (1974) *Bacteriol. Rev.* **38,** 87–110
23. De Petris, S. (1967) *J. Ultrastruct. Res.* **19,** 45–83
24. Strauss, J., Burnham, N. A., and Camesano, T. A. (2009) *J. Mol. Recognit.* **22,** 347–355
25. Liu, D., and Reeves, P. R. (1994) *Microbiology* **140,** 49–57
26. Shroll, R. M., and Straatsma, T. P. (2002) *Biopolymers* **65,** 395–407
27. Yao, X., Jericho, M., Pink, D., and Beveridge, T. (1999) *J. Bacteriol.* **181,** 6865–6875
28. Baba, T., Ara, T., Hasegawa, M., Takai, Y., Okumura, Y., Baba, M., Datsenko, K. A., Tomita, M., Wanner, B. L., and Mori, H. (2006) *Mol. Systems Biol.* **2,** 2006.0008
29. Bielig, H., Rompikuntal, P. K., Mitesh D., Zurek, B., Lindmark, B., Ramstedt, M., Wai, S. N., and Kufer, T. A. (2011) *Infect. Immun.*, in press
30. Mekalanos, J. J. (1983) *Cell* **35,** 253–263